Identification of Systems with Limit Cycles[1]

Seth L. Lacy
Air Force Research Lab, Space Vehicles
Kirtland AFB NM 87117
seth.lacy@kirtland.af.mil

Dennis S. Bernstein
Aerospace Engineering, University of Michigan
Ann Arbor MI 48109
dsbaero@umich.edu

Abstract

Limit cycle oscillations occur in a wide range of electrical, mechanical, and aerospace applications. In this paper we present a method for constructing system models that are able to reproduce a periodic signal as a limiting trajectory. Our approach is based on continuous-time modeling of a scalar nth-order system whose dynamics are represented as a map of integrals and derivatives of the available signal. The method is demonstrated on the classical Van der Pol oscillator and a nonlinear oscillator with piecewise linear damping.

1 Introduction

Roughly speaking, a limit cycle is a stable, sustained oscillation occurring in a self-excited or self-oscillating system [1, 17]. This behavior is of interest for two distinct reasons. First, although sustained oscillations can occur in linear systems such as the Lyapunov stable system

$$\ddot{q}(t) + q(t) = 0, \tag{1.1}$$

this oscillation is not stable in the sense that a small perturbation can cause the oscillation to grow or decay. Furthermore, the system

$$\dot{q}(t) + q(t) = \sin t \tag{1.2}$$

can experience sustained oscillations due to time-dependent forcing, while the system

$$\ddot{q}(t) + (\sin \omega t)q(t) = 0 \tag{1.3}$$

can possess sustained oscillation through parametric excitation. In contrast, limit cycle oscillations can occur in systems that have no time dependence in terms of either an exogenous input or internal dynamics.

Clearly, systems with limit cycles must have a source of energy to possess sustained oscillations, and this source of energy may appear in the form of a constant input. For example, the scalar system

$$\dot{q}(t) = \alpha, \tag{1.4}$$

$$y(t) = \sin q(t), \tag{1.5}$$

with constant input α possesses the limiting periodic solution $y(t) = \sin[\alpha t + q(0)]$. In this case the periodicity is due to the nonlinear output map rather than nonlinear dynamics per se. However, like the system (1.1), this system lacks structural stability. Of greater interest is the classical Van der Pol oscillator with dynamics

$$\ddot{q}(t) + (q^2(t) - 1)\dot{q}(t) + q(t) = 0 \tag{1.6}$$

which is autonomous and whose limit cycle is robust to perturbations in the damping and stiffness terms.

Limit cycles arise in a wide range of applications. Van der Pol himself analyzed the self-excited oscillations of the positive feedback amplifier, an invention of extreme technological importance. Furthermore, limit cycle dynamics occur in mechanical systems with autoparametric vibrations, such as the rotational dynamics of unbalanced rigid and flexible rotors [14, 15, 23]. Additional applications include acoustic-combustion dynamics where heat release excites acoustic dynamics [13, 18, 21] as well as fluid-structure interaction, which can give rise to the instability known as flutter [2, 3, 8, 10, 12, 19, 22]. An interesting application of limit cycle dynamics is the artificial generation of musical instrument sounds [7, 16]. Identification of limit cycle dynamics has been studied in [5].

The mathematics of limit cycle dynamics were first studied by Poincare in the 1880's. The difficulty of the problem is suggested by Hilbert's 16th problem which concerned the maximum number of limit cycles of planar systems with quadratic dynamics. While existence and properties of limit cycles in planar systems remains a research problem of intense current interest [24], the study of limit cycles in higher dimensions is largely unstudied, presumably due to the difficulty of the problem as well as the emphasis on chaotic motion which can occur in dimension 3 or higher. Likewise, there has been little study of limit cycles in discrete-time systems, where chaos can occur in first-order systems.

Despite these difficulties there is intense interest in constructing systems to reproduce limit cycle behavior. One of the prime motivations for this interest is the potential usefulness in using the model to understand the internal dynamics of complex systems. For example, models are constructed in [11] to reproduce the dynamics of a heart as measured by an electrocardiogram. In the systems literature the limit cycle identification problem is a blind nonlinear identification problem [21], whereas in the physics and mathematics literature this is a problem of vector field reconstruction or restoration [4, 9, 11].

In the present paper we extend the method of [11] by constructing a nonlinear system to reproduce a periodic signal as a limiting trajectory. Our approach is based on continuous-time modeling of a scalar nth-order system whose dynamics are represented as a polynomial map of integrals and derivatives of the available signal. Least-squares methods are then used to determine the

[1]This research was supported by NASA under GSRP NGT4-52421 and AFOSR under grant F49620-01-1-0094 and laboratory research initiative 00VS17COR.

unknown coefficients. The method is demonstrated on the classical Van der Pol oscillator as well as a nonlinear oscillator with piecewise linear damping.

2 Problem Formulation

We begin with periodic scalar output data collected from a system with a limit cycle and no observed input. We use a single period of data for our identification. Explicitly, we are given a function $y(t)$ defined for $t_i \leq t \leq t_f$. The goal is to construct a system whose output $\hat{y}(t)$ converges to $y(t)$ as $t \to \infty$. Since phase is not of concern to us, it suffices to perform the identification such that, for a specified $\epsilon > 0$, there exists $\alpha \in [0, T]$, $T = t_f - t_i$, such that

$$\lim_{k\to\infty} \sup_{t\in[0,T]} |\hat{y}(t + kT + \alpha) - y(t)| < \epsilon, \tag{2.1}$$

where k denotes a positive integer.

If we look for continuous-time systems with nonlinear output equations we can proceed as follows. We write the differential equation for the elliptical limit cycle [20]

$$\dot{x}_1 = x_2 \tag{2.2}$$

$$\dot{x}_2 = \lambda a^2 x_2 - \frac{\lambda}{\omega^2} x_2^3 - \lambda x_1^2 x_2 - \omega^2 x_1 \tag{2.3}$$

with $\lambda = a = \omega = 1$. x_1 converges to a sinusoidal output with amplitude a and frequency ω. λ determines the speed of convergence. We re-scale time and append an output equation to obtain

$$\dot{x}_1 = \frac{2\pi}{T} x_2 \tag{2.4}$$

$$\dot{x}_2 = \frac{2\pi}{T} \left(x_2 - x_2^3 - x_1^2 x_2 - x_1 \right) \tag{2.5}$$

$$\hat{y} = h(\frac{T}{2\pi} (\angle(x_2 + i x_1) + \pi)). \tag{2.6}$$

While the above approach can reproduce arbitrary limit cycles to within a phase shift, it provides no useful information about the dynamics of the original system. Hence we limit ourselves to systems with linear output equations. Assuming that y is differentiable, a simple candidate for this approach is

$$\dot{\hat{y}} = \dot{y}(\mathrm{rem}(t, T)). \tag{2.7}$$

which integrates to

$$\hat{y} = y(\mathrm{rem}(t, T)) + c, \tag{2.8}$$

where $\mathrm{rem}(t, T)$ gives the remainder of t/T and c is chosen by the user. Now the phase of the limit cycle is correct, but there is an offset error determined by c. This system doesn't tell us anything about the underlying dynamics of the original system. Therefore, we restrict our attention to time-invariant continuous-time systems with linear output equations.

If the solution to a second order continuous-time system remains bounded, then either the solution approaches an equilibrium, or the solution approaches a limit cycle. There are no chaotic solutions in the two-dimensional case [6]. On the other hand, higher dimensional systems may be chaotic. Thus, if the order of the system is unknown, it makes sense to first identify a two-dimensional model, and resort to higher order models only if this fails.

We consider systems of the form

$$y^{(n)} = F(y^{(n-1)}, \ldots, \dot{y}, y, \textstyle\int y, \cdots y^{(-m)}), \tag{2.9}$$

where

$$F(y^{(n-1)}, \ldots, \dot{y}, y, \textstyle\int y, \ldots, y^{(-m)}) = \sum_{i=1}^{N} c_i f_i(y^{(n-1)}, \ldots, \dot{y}, y, \textstyle\int y, \ldots, y^{(-m)}) = c^{\mathrm{T}} f, \tag{2.10}$$

$f \triangleq \begin{bmatrix} f_1 & \cdots & f_N \end{bmatrix}^{\mathrm{T}} : \mathbb{R}^{m+n} \to \mathbb{R}^N$, $f_i : \mathbb{R}^{m+n} \to \mathbb{R}$, $F : \mathbb{R}^{m+n} \to \mathbb{R}$, and $f_1, \ldots, f_N$ is a linearly independent set of known basis functions with unknown coefficients $c \triangleq \begin{bmatrix} c_1 & \cdots & c_N \end{bmatrix}^{\mathrm{T}}$. In particular we want to consider second-order systems of the form (2.9).

To obtain an estimate $\hat{c}$ of c we minimize the L_2 norm cost function

$$J(c) = \left\| y^{(n)} - c^{\mathrm{T}} f \right\|_2^2 = \int_{t_i}^{t_f} \left(y^{(n)} - c^{\mathrm{T}} f \right)^2 dt. \tag{2.11}$$

The derivative of J is given by

$$\begin{aligned} \frac{\partial J}{\partial c} &= -2 \int_{t_i}^{t_f} \left(y^{(n)} - c^{\mathrm{T}} f \right) f \, dt \\ &= 2 \int_{t_i}^{t_f} f f^{\mathrm{T}} c - y^{(n)} f \, dt \\ &= 2 \left(\int_{t_i}^{t_f} f f^{\mathrm{T}} \, dt \; c - \int_{t_i}^{t_f} y^{(n)} f \, dt \right), \end{aligned} \tag{2.12}$$

so the minimizer of J is given by

$$\hat{c} = \left(\int_{t_i}^{t_f} f f^{\mathrm{T}} \, dt \right)^{-1} \int_{t_i}^{t_f} y^{(n)} f \, dt, \tag{2.13}$$

where the inverse of the matrix $\int_{t_i}^{t_f} f f^{\mathrm{T}} \, dt$ exists because the basis functions are assumed to be linearly independent.

3 Van der Pol Oscillator

We consider the Van der Pol oscillator

$$\ddot{q} = -\omega^2 q + \epsilon\omega(1 - \mu^2 q^2)\dot{q}, \tag{3.1}$$

where $\omega = \epsilon = \mu = 1$. We investigate how the choice of the measured signal affects the performance of the method. For both choices of measurement ($y = q$ and $y = \dot{q}$) we consider different combinations of integration and differentiation.

3.1 Measure $y = q$

We take $y(t) = q(t)$ as our measurement and collect one period of data after the output has converged to the limit cycle, see Figure 2.

3.1.1 Differentiate Twice

We differentiate y twice to obtain $\dot{y}$ and $\ddot{y}$. We select all polynomials up to cubic order in y and $\dot{y}$ for

our linearly independent basis functions,

$$f = \begin{bmatrix} 1 & y & \dot{y} & y^2 & \dot{y}^2 & y\dot{y} & y^2\dot{y} & y\dot{y}^2 & y^3 & \dot{y}^3 \end{bmatrix}^{\mathrm{T}}. \quad (3.2)$$

Equation (2.13) then yields

$$\hat{c} = \left(\int_{t_i}^{t_f} f f^{\mathrm{T}} \, dt \right)^{-1} \int_{t_i}^{t_f} \ddot{y} f \, dt$$
$$= \begin{bmatrix} 0 & -1.00 & 1.00 & 0 & 0 & 0 & -1.00 & 0 & 0 & 0 \end{bmatrix}^{\mathrm{T}}. \quad (3.3)$$

The error in the estimate of c is

$$e_c = \frac{\|\hat{c} - c\|}{\|c\|}, = 0.0007. \quad (3.4)$$

and the error in the limit cycle is

$$e_q = \sqrt{\frac{\int_{t_i}^{t_f} (\hat{y} - y)^2 \, dt}{\int_{t_i}^{t_f} y^2 \, dt}} = 0.0013. \quad (3.5)$$

3.1.2 Integrate Once and Differentiate Once

Now we integrate the measurement $y(t) = q(t)$ once and differentiate it once to obtain the three necessary signals, instead of differentiating it twice as above. We select all polynomials up to cubic order in $\int y$ and y for our linearly independent basis functions,

$$f = [\ 1 \quad \int y \quad y \quad (\int y)^2$$
$$y^2 \quad \int yy \quad (\int y)^2 y \quad \int yy^2 \quad (\int y)^3 \quad y^3 \ ]^{\mathrm{T}}. \quad (3.6)$$

Equation (2.13) then yields

$$\hat{c} = \left(\int_{t_i}^{t_f} f f^{\mathrm{T}} \, dt \right)^{-1} \int_{t_i}^{t_f} \dot{y} f \, dt$$
$$= \begin{bmatrix} 0.33 & -1.00 & 1.00 & 0 & 0 & 0 & 0 & 0 & 0 & -0.33 \end{bmatrix}^{\mathrm{T}}. \quad (3.7)$$

This is roughly

$$\ddot{y} = \frac{1}{3} - y + \dot{y} - \frac{1}{3}\dot{y}^3, \quad (3.8)$$

which can be differentiated to obtain

$$\dddot{y} = -\dot{y} + \ddot{y} - \dot{y}^2 \ddot{y}, \quad (3.9)$$
$$\ddot{z} = -z + \dot{z} - z^2 \dot{z}, \quad (3.10)$$

identifying $z = \dot{y}$. Hence we have obtained the original differential equation.

The error in the limit cycle is

$$e_q = \sqrt{\frac{\int_{t_i}^{t_f} (\hat{y} - y)^2 \, dt}{\int_{t_i}^{t_f} y^2 \, dt}} = 0.0001. \quad (3.11)$$

3.1.3 Integrate Twice

Now we integrate the measurement $y = q$ twice to obtain the three necessary signals. We select all polynomials up to cubic order in $\int y$ and $\int \int y$ for our linearly independent basis functions,

$$f = [\ 1 \quad \int\int y \quad \int y \quad (\int\int y)^2 \quad (\int y)^2 \quad \int\int y \int y$$
$$(\int\int y)^2 \int y \quad \int\int y (\int y)^2 \quad (\int\int y)^3 \quad (\int y)^3 \ ]^{\mathrm{T}}. \quad (3.12)$$

Unfortunately, this set of basis functions is linearly dependent. We only discover this when checking the rank of $\int_{t_i}^{t_f} f f^{\mathrm{T}} \, dt$.

3.2 Measure $y = \dot{q}$

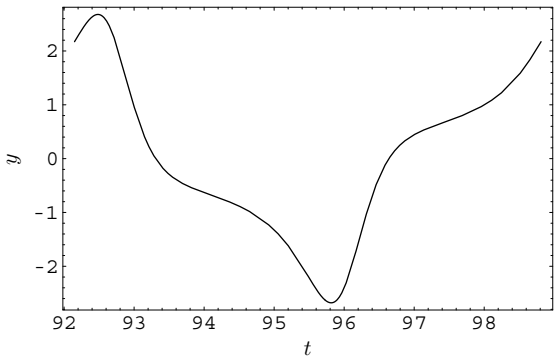

Figure 1: Measurement $y = \dot{q}$ over one period

We take $y(t) = \dot{q}(t)$ as our measurement and collect one period of data after the output has converged to the limit cycle, see Figure 1.

3.2.1 Differentiate Twice

We differentiate y twice to obtain $\dot{y}$ and $\ddot{y}$. We select all polynomials up to cubic order in y and $\dot{y}$ for our linearly independent basis functions (3.2). Equation (2.13) then yields

$$\hat{c} = \left(\int_{t_i}^{t_f} f f^{\mathrm{T}} \, dt \right)^{-1} \int_{t_i}^{t_f} \ddot{y} f \, dt$$
$$= \begin{bmatrix} 0 & 4.19 & -3.48 & 0 & 0 & 0 & 0.96 & 0.19 & -1.38 & 0.13 \end{bmatrix}^{\mathrm{T}}. \quad (3.13)$$

The error in the limit cycle is

$$e_q = \sqrt{\frac{\int_{t_i}^{t_f} (\hat{y} - y)^2 \, dt}{\int_{t_i}^{t_f} y^2 \, dt}} = 1.5731. \quad (3.14)$$

We note that the identification model can not capture the true dynamics. On the other hand, the identified model does have a limit cycle. However, for this example, the limit cycle of the identified model does not approximate the measured limit cycle well.

3.3 Adding Disturbances

One way to perturb this continuous time system is to degrade the accuracy of the initial solution, the data. We perform the numerical integration in the simulation with only two digits of accuracy and obtain one period of the limit cycle, here compared to the high-accuracy (twenty digits of accuracy) "true" data, see Figure 2. The error introduced is

$$e_{\mathrm{approx}} = \sqrt{\frac{\int_{t_i}^{t_f} (y - y_{\mathrm{true}})^2 \, dt}{\int_{t_i}^{t_f} y_{\mathrm{true}}^2 \, dt}} = 0.03857. \quad (3.15)$$

We then differentiate the low-accuracy data twice and identify a model using the basis functions (3.2). We obtain an estimate of the model given by

$$\hat{c} = \left(\int_{t_i}^{t_f} f f^{\mathrm{T}} \, dt \right)^{-1} \int_{t_i}^{t_f} \ddot{y} f \, dt$$
$$= \begin{bmatrix} 0 & -1.03 & 0.85 & 0 & 0 & 0 & -0.90 & 0.02 & 0.01 & 0 \end{bmatrix}^{\mathrm{T}}. \quad (3.16)$$

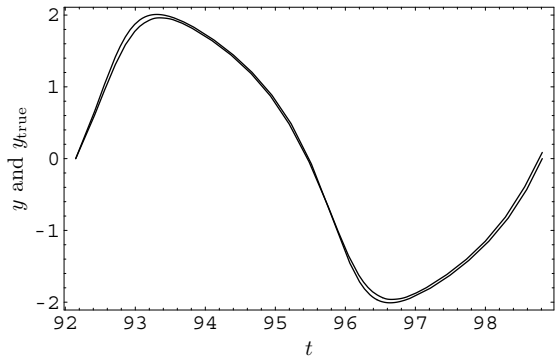

Figure 2: y and y_{true}

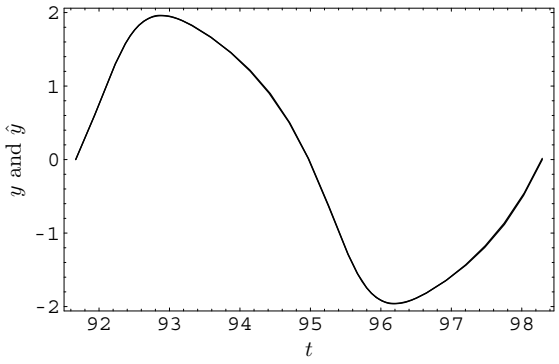

Figure 3: y and $\hat{y}$

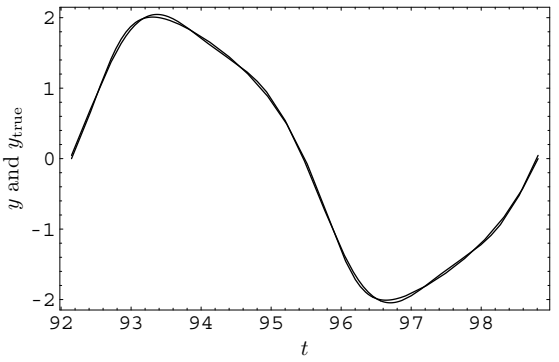

Figure 4: y and y_{true}

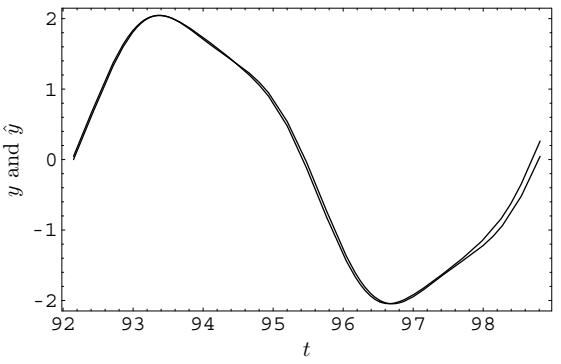

Figure 5: y and $\hat{y}$ for the Trigonometric Approximation Example

This differs from the true coefficients by

$$e_c = \frac{\|\hat{c} - c\|}{\|c\|} = 0.1060, \tag{3.17}$$

about 10%.

We compare the limit cycle of the identified model to the measured degraded limit cycle, see Figure 3. The error in the limit cycle is

$$e_q = \sqrt{\frac{\int_{t_i}^{t_f} (\hat{y} - y)^2 \, dt}{\int_{t_i}^{t_f} y^2 \, dt}} = 0.006396 \tag{3.18}$$

still very good. With the degraded initial data, the algorithm produced a system with a limit cycle matching the degraded signal well.

A second source of error occurs when we approximate the data with trigonometric functions, as in

$$y(t) = a_1 + \sum_{i=1}^{M} a_{2i} \sin\left(\frac{2\pi i}{T} t\right) + a_{2i+1} \cos\left(\frac{2\pi i}{T} t\right). \tag{3.19}$$

The derivatives of y are given by

$$y^{(n)}(t) = \sum_{i=1}^{M} \left(\frac{2\pi i}{T}\right)^n (-1)^{n(n-1)/2} \times \left(a_{2i} \sin\left(\frac{2\pi i}{T} t\right) + (-1)^n a_{2i+1} \cos\left(\frac{2\pi i}{T} t\right)\right). \tag{3.20}$$

We compare the original data to it's trigonometric approximation with $M = 3$, see Figure 4. The error introduced is

$$e_{\text{trig}} = \sqrt{\frac{\int_{t_i}^{t_f} (y - y_{\text{true}})^2 \, dt}{\int_{t_i}^{t_f} y_{\text{true}}^2 \, dt}} = 0.02429. \tag{3.21}$$

We differentiate the trigonometric function y twice and identify a model using the basis functions (3.2). We obtain an estimate of the model given by

$$\hat{c} = \left(\int_{t_i}^{t_f} f f^{\mathrm{T}} \, dt\right)^{-1} \int_{t_i}^{t_f} \ddot{y} f \, dt$$
$$= \begin{bmatrix} 0 & 2.15 & 5.63 & 0 & 0 & 0 & -1.85 & 0.08 & -0.84 & -0.95 \end{bmatrix}^{\mathrm{T}}. \tag{3.22}$$

This differs from the true coefficients by

$$e_c = \frac{\|\hat{c} - c\|}{\|c\|} = 3.3493, \tag{3.23}$$

about 335%!

We compare the limit cycle of the identified model to the measured limit cycle, see Figure 5. The error in the limit cycle is

$$e_q = \sqrt{\frac{\int_{t_i}^{t_f} (\hat{y} - y)^2 \, dt}{\int_{t_i}^{t_f} y^2 \, dt}} = 0.04718, \tag{3.24}$$

still very good. Although the initial data was degraded by approximating it with only a few sinusoids, the algorithm produced a system with a limit cycle matching the trigonometric signal well.

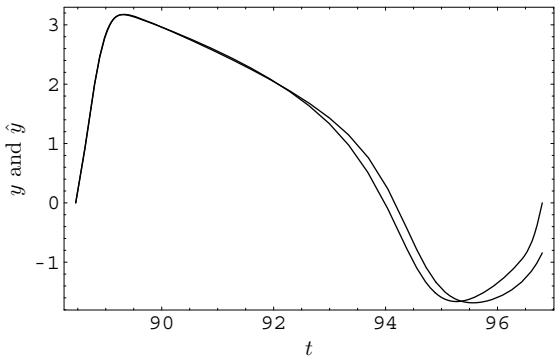

Figure 6: Piecewise Linear Limit Cycle and the Identified Limit Cycle

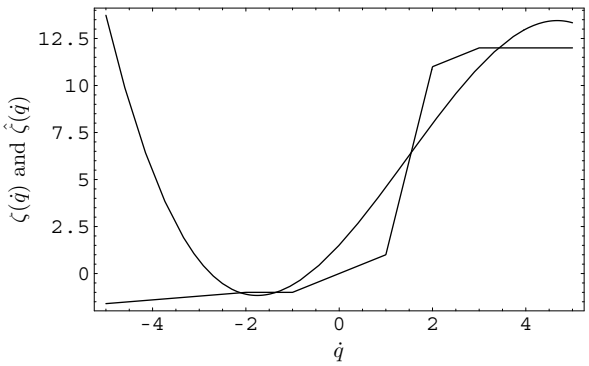

Figure 7: Piecewise Linear Damping Function and the Identified Polynomial Damping Function

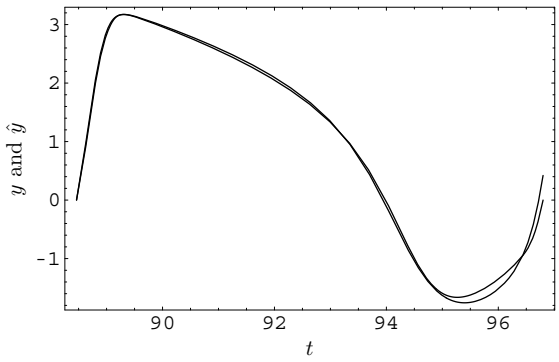

Figure 8: Piecewise Linear Limit Cycle and the Identified Limit Cycle

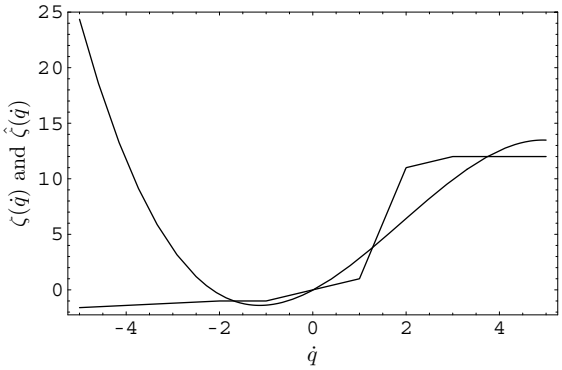

Figure 9: Piecewise Linear Damping Function and the Identified Polynomial Damping Function

4 Piecewise Linear Damping

Here we examine the system

$$\ddot{q} = -q + \zeta(\dot{q}) - q^2\dot{q}, \tag{4.1}$$

where $\zeta : \mathbb{R} \to \mathbb{R}$ is the piecewise linear function shown in Figure 7. Note that we recover the Van Der Pol equation if $\zeta(\dot{q}) = \dot{q}$. We measure $y(t) = q(t)$, see Figure 6, and use (3.2) as our basis functions. We recover

$$\hat{c} = \left(\int_{t_i}^{t_f} f f^{\mathrm{T}}\, dt\right)^{-1} \int_{t_i}^{t_f} \ddot{y} f\, dt = [1.51\ \ -0.42$$
$$2.71\ -0.36\ \ 0.48\ \ 0.57\ -1.13\ -0.05\ \ 0.02\ -0.11]^{\mathrm{T}}. \tag{4.2}$$

We compare the limit cycle of identified model to the measured limit cycle in Figure 6. The identified model has a limit cycle with a slightly longer period. The error in the limit cycle is

$$e_q = \sqrt{\frac{\int_{t_i}^{t_f} (\hat{y} - y)^2\, dt}{\int_{t_i}^{t_f} y^2\, dt}} = 0.0986. \tag{4.3}$$

We compare $\zeta(\dot{q})$ to $\hat{\zeta}(\dot{q}) = \hat{c}_1 + \hat{c}_3\dot{q} + \hat{c}_5\dot{q}^2 + \hat{c}_{10}\dot{q}^3$ in Figure 7.

Next we use

$$f = \begin{bmatrix} 1 & y & \dot{y} & \dot{y}^2 & y^2\dot{y} & \dot{y}^3 \end{bmatrix}^{\mathrm{T}} \tag{4.4}$$

as our basis functions. We recover

$$\hat{c} = \left(\int_{t_i}^{t_f} f f^{\mathrm{T}}\, dt\right)^{-1} \int_{t_i}^{t_f} \ddot{y} f\, dt$$
$$= \begin{bmatrix} -0.03 & -0.82 & 2.24 & 0.76 & -0.99 & -0.13 \end{bmatrix}. \tag{4.5}$$

We compare the limit cycle of identified model to the measured limit cycle in Figure 8. The identified model has a limit cycle with a slightly longer period. The error in the limit cycle is

$$e_q = \sqrt{\frac{\int_{t_i}^{t_f} (\hat{y} - y)^2\, dt}{\int_{t_i}^{t_f} y^2\, dt}} = 0.0409 \tag{4.6}$$

We compare $\zeta(\dot{q})$ to $\hat{\zeta}(\dot{q}) = \hat{c}_1 + \hat{c}_3\dot{q} + \hat{c}_4\dot{q}^2 + \hat{c}_6\dot{q}^3$ in Figure 9. The method seems to perform well even when the true dynamics cannot be represented by the basis functions well.

5 Conclusion

We developed a method for identifying systems with limit cycles. We use one period of data to identify the limit cycle dynamics. Our approach is to identify a continuous time model whose dynamics are functions of the measured signal, derivatives of the measured signal, and integrals of the measured signal. We demonstrated the method on the Van Der Pol oscillator, as well as an oscillator with a piecewise linear term. We considered

perturbations of the original data by reducing numerical accuracy, and by approximating the data with trigonometric functions. We found that the performance of the method depends on whether the original differential equation can be modeled using the proposed structure. We also found that the method does not critically depend on the basis functions used to approximate the system dynamics. Future work will focus on methods for basis function selection and experimental applications.

References

[1] A. A. Andronov, A. A. Vitt, and S. E. Khaikin. *Theory of Oscillators*. Dover, 1987. reprint.

[2] R. L. Bisplinghoff and H. Ashley. *Principles of Aeroelasticity*. Wiley, 1962.

[3] R. D. Blevins. *Flow-Induced Vibration*. Van Nostrand Reinhold, 1990.

[4] J. L. Breeden and A. Hubler. Reconstructing equations of motion from experimental data with unobserved variables. *Physical Rev. A*, 42:5817–5826, 1998.

[5] R. A. Casas, R. R. Bitmead, C. A. Jacobson, and C. R. Johnson, Jr. Prediction error methods for limit cycle data. *Automatica*, 38(10):1753–1760, October 2002.

[6] P. G. Drazin. *Nonlinear Systems*. Cambridge Texts in Applied Mathematics. Cambridge University Press, 1992.

[7] N. H. Fletcher and T. D. Rossing. *The Physics of Musical Instruments*. Springer, 1991.

[8] Y. C. Fung. *An Introduction to the Theory of Aeroelasticity*. Wiley, 1955.

[9] G. Gouesbet and C. Letellier. Global vector-field reconstruction by using a multivariable polynomial l_2 approximation on nets. *Physical Rev. E*, 49:4955–4972, 1998.

[10] M. S. Howe. *Acoustics of Fluid-Structure Interactions*. Cambridge University Press, 1998.

[11] N. B. Janson, A. N. Pavlov, and V. S. Anishchenko. One method for restoring inhomogeneous attractors. *Int. J. Bifurcation and Chaos*, 8:825–833, 1998.

[12] J. Ko et al. Structured model reference adaptive control for a wing section with structural nonlinearity. *Journal of Vibration Control*, 8:553–573, 2002.

[13] S. L. Lacy, R. Venugopal, and D. S. Bernstein. Armarkov adaptive control of self-excited oscillations of a ducted flame. In *Proceedings of the 37th Conference on Decision and Control*, Tampa Florida, December 1998.

[14] K.-Y. Lum, S. P. Bhat, V. T. Coppola, and D. S. Bernstein. Adaptive virtual autobalancing for a magnetic rotor with unknown mass imbalance: Theory and experiment. *Transactions of the ASME, Journal of Vibration and Acoustics*, 120(2):557–570, April 1998.

[15] K.-Y. Lum, V. T. Coppola, and D. S. Bernstein. Adaptive autocentering control for an active magnetic bearing supporting a rotor with unknown mass imbalance. *IEEE Transactions on Control Systems Technology*, 4:587–597, 1996.

[16] M. E. McIntyre, R. T. Shumacher, and J. Woodhouse. On the oscillations of musical instruments. *Journal of the Acoustic Society of America*, 74:1325–1345, 1983.

[17] N. Minorsky. *Nonlinear Oscillations*. Van Nostrand, Princeton, 1962. reprint.

[18] R. M. Murray et al. System identification for limit cycling systems: A case study for combustion instabilities. In *Proceedings of the American Control Conference*, pages 2004–2008, Philadelphia, PA, June 1998.

[19] D. Rockwell and E. Naudascher. Review–self-sustaining oscillations of flow past cavities. *Journal of Fluids Engineering*, 100:152–165, 1978.

[20] A. V. Roup and D. S. Bernstein. Stabilization of a class of nonlinear systems using direct adaptive control. *IEEE Transactions on Automatic Control*, 46:1821–1825, 2001.

[21] S. M. Savaresi, R. R. Bitmead, and W. J. Dunstan. Nonlinear system identification using closed-loop data with no external excitation: The case of a lean combustion chamber. *Int. J. Contr.*, 74:1796–1806, 2001.

[22] A. Tondl, T. Ruijgrok, F. Verhulst, and R. Nabergoj. *Autoparametric Resonance in Mechanical Systems*. Cambridge, 2000.

[23] C.-J. Wan, D. S. Bernstein, and V. T. Coppola. Global stabilization of the oscillating eccentric rotor. *Nonlinear Dynamics*, 10:49–62, 1996.

[24] Y. Yan-Qian. *Theory of Limit Cycles*, volume 66 of *Translations of Mathematical Monographs*. American Mathematical Society, second edition, 1986.